

Synthesis and Characterization of Colorless Polyimides Derived from 4-(4-Aminophenoxy)-2,6-dimethylaniline

Sehwa Bong^{1,2}, Hyeonuk Yeo¹, Munju Goh¹, Bon-Cheol Ku¹, Yoo Young Kim², Pill-Hoon Bong², Byoungnam Park³, and Nam-Ho You^{*1}

¹Carbon Composite Materials Research Center, Institute of Advanced Composites Materials, Korea Institute of Science and Technology, Eunha-ri san 101, Bondong-eup, Wanju-gun, Jeonbuk 55324, Korea

²Department of Carbon Fusion Engineering, Jeonju University, 45 Baengma-gil, Wansan-gu, Jeonju, Jeonbuk 55069, Korea

³Department of Materials Science and Engineering, Hongik University 72-1, Sangsu-dong, Mapo-gu, Seoul 04066, Korea

Received July 15, 2016; Revised September 22, 2016; Accepted September 30, 2016

Abstract: A new aromatic polyimides (PIs) having asymmetric aromatic diamine with methyl groups at the *ortho* position of amino group has been developed to prepare transparent film in the visible region. The all aromatic PIs presented here are derived from 4-(4-aminophenoxy)-2,6-dimethylaniline (APDMA) and aromatic dianhydride, 4,4'-(hexafluoroisopropylidene)diphthalic anhydride (6FDA), 4,4'-oxydiphthalic anhydride (ODPA), 4,4'-biphenalic anhydride (BPDA), and pyromellitic dianhydride (PMDA) via a two-step polycondensation. All PIs show good thermal properties: 5% weight loss at a temperature range of 510–529 °C and their glass transition temperature found above 290 °C. The PIs exhibit good optical transparency, such as cut-off wavelength in the region of 296–358 nm and above 92–99% at 550 nm. In addition, all PIs show low refractive indices in the range of 1.567–1.637 at wavelength of 637 nm and low birefringence.

Keywords: films, polyimide, dimethyl groups, refractive index, birefringence, polymer optics.

Introduction

In recent years, thermally stable and optically transparent polymers have found wide application to various optoelectronic components such as plastic substrates, color filters, roll-up displays, and portable devices.¹ In particular, aromatic polyimides (APIs) are one of the few high performance polymers that possess various outstanding properties, such as excellent thermal dimensional stability, adhesion to metal, chemical resistance, and low dielectric constant.² Therefore, much attention has been focused on the application of APIs for optical and electronic devices. However, APIs show strong absorption in the visible region originating from the formation of charge-transfer complex (CTC) between electron donor and electron acceptor in the polymers, which can disturb their optical applications.³

The general approach to improve optical transparency of polyimides is the introduction of substituents, such as fluorinated components, flexible linkages, bulky substituents, and alicyclic moieties.⁴ Although the incorporation of flexible linkages and fluorinated substituents in polyimide backbone can improve optical transparency, their mechanical and thermal properties, such as glass transition temperature and coefficient of

thermal expansion (CTE), are decreased due to the decrease of the APIs' packing density.⁵ In contrast, the introduction of large pendant or unsymmetrical groups in the APIs backbone is a relatively effective way to enhance optical transparency while maintaining thermal properties.⁶

In this study, we report effective ways to improve optical transparency and thermal properties simultaneously in the APIs. The new asymmetric aromatic diamine, 4-(4-aminophenoxy)-2,6-dimethylaniline (APDMA), was designed and synthesized to prepare APIs with commercial aromatic dianhydrides, such as 4,4'-(hexafluoroisopropylidene)diphthalic anhydride (6FDA), 4,4'-oxydiphthalic anhydride (ODPA), 4,4'-biphenalic anhydride (BPDA), and pyromellitic dianhydride (PMDA). The asymmetric aromatic diamine with methyl groups at the *ortho* position of amino group can not only improve optical transparency because of a twisted structure between C-N imide bonds which reduces CTC but also enhances the glass transition temperature because the methyl groups increase chain rigidity in APIs, preventing free rotation of the C-N imide bond.⁷ Moreover, the new diamine induces a low-dielectric constant and refractive index for APIs. The structure-property relationships, thermal properties, and dielectric constant of the APIs are investigated in detail.

*Corresponding Author. E-mail: polymer@kist.re.kr

Experimental

Measurements. ^1H (600 MHz) and ^{13}C (150 MHz) NMR spectra were recorded on an Agilent 600 MHz Premium COMPACT NMR spectrometer. ^1H and ^{13}C NMR spectra were obtained by using tetramethylsilane (TMS) as an internal standard and CDCl_3 as a solvent. The functional surface groups of the polymer film were analyzed by using a Fourier transform-infrared spectroscopy (FTIR Spectrophotometer, Nicolet IS10, USA). Thermogravimetric analysis (TGA) was carried out with a TA 50 (TA Instruments, USA) under nitrogen gas flow at a heating rate of 10 $^\circ\text{C}/\text{min}$. Glass transition temperatures of the synthetic compounds were measured by DSC analysis with a Q 20 (TA Instruments, USA) under nitrogen gas flow at a heating rate of 10 $^\circ\text{C}/\text{min}$. Dynamic mechanical thermal analysis (DMA) was evaluated from PI films (30 mm length, 5 mm wide, and *ca.* 60 μm thickness) on a DMA (TA Instruments, DMA Q 800, USA) at a heating rate of 3 $^\circ\text{C}/\text{min}$ with a load frequency of 1 Hz in air. The UV-visible spectra were recorded on a JASCO V-670 spectrometer. The out-of-plane (n_{TM}) and in-plane (n_{TE}) refractive indices of polymer films were measured with a Metricon PC-2000 prism coupler with a He-Ne laser light source (wavelength: 637 nm). The birefringence (Δn) was calculated to measure the difference between n_{TE} and n_{TM} . The average refractive index was calculated according to the equation: $n_{av} = [(2n_{TE}^2 + n_{TM}^2)/3]^{1/2}$.

Materials. 4-Amino-3,5-xylenol and 1-chloro-4-nitrobenzene were obtained from TCI and Sigma-Aldrich and were used without further purification. Aromatic dianhydrides, 4,4'-(hexafluoroisopropylidene)diphthalic anhydride (6FDA), 4,4'-oxydiphthalic anhydride (ODPA), 4,4'-biphenalic anhydride (BPDA), and pyromellitic dianhydride (PMDA) were purchased from TCI and used after sublimation. Dimethylformamide (DMF) and *N*-methyl-2-pyrrolidone (NMP) were purified by a two-column solid-state purification system (Glass contour system, Joerg Meyer, Irvine, CA). All reactions were performed under an argon atmosphere.

Monomer Synthesis.

Synthesis of 2,6-Dimethyl-4-(4-nitrophenoxy)aniline (DMNPA). 4-Amino-3,5-xylenol (10.0 g, 72.9 mmol), 1-chloro-4-nitrobenzene (11.5 g, 72.9 mmol), K_2CO_3 (15.0 g, 109.4 mmol), and 150 mL of dimethylformamide (DMF) were mixed. The solution was stirred at 120 $^\circ\text{C}$ for 12 h under Ar atmosphere. The product was poured into brine and extracted with ethyl acetate, after drying over MgSO_4 , and solvent was removed under vacuum. The product was purified by silica gel chromatography (ethyl acetate:hexane=1:5, $R_f=0.3$) and recrystallization in dichloromethane. The product DMNPA (13.5 g, 52.2 mmol, 71% yield) was obtained as a brown solid. m.p.: 109.7 $^\circ\text{C}$, ^1H NMR (600 MHz, CDCl_3): $\delta=8.16$ (d, $J=9.3$ Hz, 2H), 6.95 (d, $J=9.3$ Hz, 2H), 6.71 (s, 2H), 3.59 (s, 2H, -NH₂), 2.20 (s, 6H) ppm. ^{13}C NMR (150 MHz, CDCl_3): $\delta=164.77$, 145.51, 141.93, 140.43, 125.81, 123.33, 120.46, 116.16, 17.78

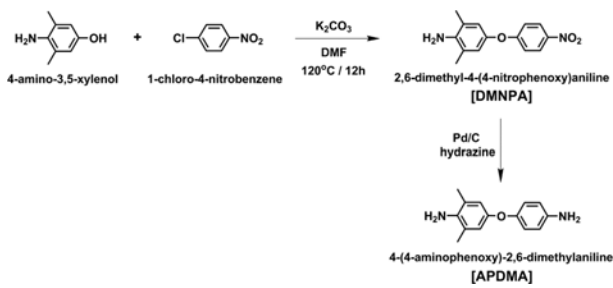
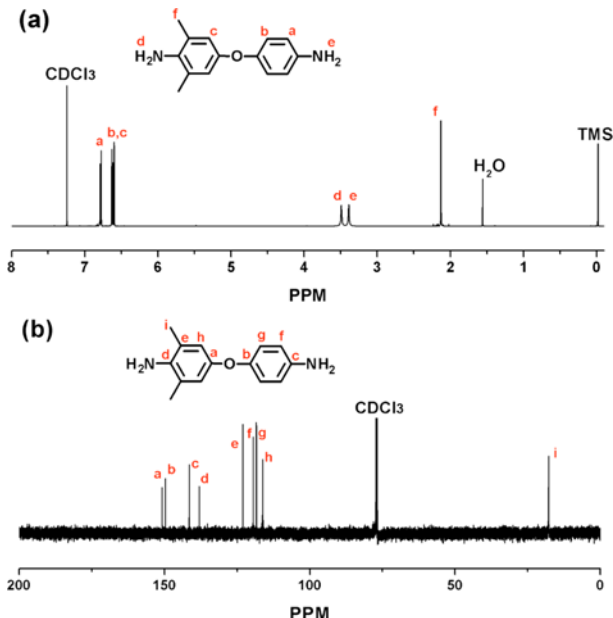
ppm. MS (+ESI): calcd for $\text{C}_{14}\text{H}_{14}\text{N}_2\text{O}_3 + \text{H}^+$: 259.10; found: 259.10.

Synthesis of 4-(4-Aminophenoxy)-2,6-dimethylaniline (APDMA): After DMNPA (13.5 g, 52.2 mmol) and 10% Pd/C (0.1 g) were dissolved in ethanol (140 mL), hydrazine (15 mL) was added by dropwise to the mixture within 1 h. After the mixture was refluxed for overnight, the solution was filtered through celite to remove Pd/C and placed in a freezer to obtain a pale-yellow crystal product APDMA (5.2 g, 22.8 mmol, 43.8% yield). m.p.: 122.6 $^\circ\text{C}$, ^1H NMR (600 MHz, CDCl_3): $\delta=6.79$ (d, $J=8.78$ Hz, 2H), 6.62 (d, $J=8.78$ Hz, 2H), 6.60 (s, 2H), 3.49 (s, 2H, -NH₂), 3.39 (s, 2H, -NH₂), 2.13 (s, 6H) ppm. ^{13}C NMR (150 MHz, CDCl_3): $\delta=150.81$, 149.72, 141.51, 138.07, 123.06, 119.52, 118.43, 116.18, 17.82 ppm. MS (API+): calcd for $\text{C}_{14}\text{H}_{16}\text{N}_2\text{O} + \text{H}^+$: 229.13; found: 229.24.

Polymer Synthesis. PI films were prepared through the traditional two-step method.⁸ First, a solution of diamine and dianhydride in equal proportion were dissolved in NMP (solid content in 16-20 wt%). The mixture was stirred for 1 day at room temperature under an argon atmosphere to acquired viscous poly(amic acid) (PAA) precursors. Second, the resulting PAA solutions were cast on the variety substrates, such as glass, quartz, and silicon wafer, and thermally imidized in curing conditions at 90 $^\circ\text{C}$ for 1 h, 150 $^\circ\text{C}$ for 1 h, 200 $^\circ\text{C}$ for 1 h, 250 $^\circ\text{C}$ for 1 h, and 300 $^\circ\text{C}$ for 30 min under Ar atmosphere. After curing, the plates were placed in water to remove substrates, and free standing flexible polyimide films were obtained. The diamine monomer APDMA was polymerized with four types of dianhydride, 6FDA, ODPA, BPDA, and PMDA, and the films were named as 6FDA-APDMA, ODPA-APDMA, BPDA-APDMA, and PMDA-APDMA, respectively. In addition, PMDA-ODA was prepared as a reference PI film. The PAA solutions were prepared as follows, diamine monomer APDMA (1.0 g, 4.4 mmol) and NMP (10.3 g, solid content in 16 wt%) were put into a 20 mL flask and stirred under an argon atmosphere. After the monomer was completely dissolved, PMDA (1.0 g, 4.4 mmol) was added in the flask. The mixed solution was stirred at room temperature for 1 day to gain a viscous PAA solution. Other PAA solutions were prepared in a similar method and their inherent viscosities measured in NMP at 30 $^\circ\text{C}$ were 0.77-1.52 dL/g.

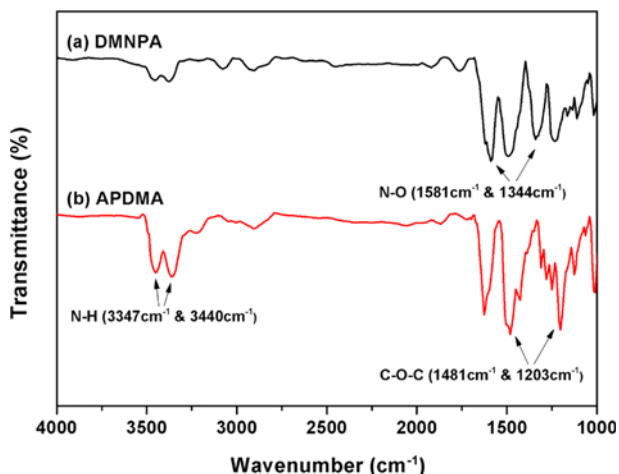
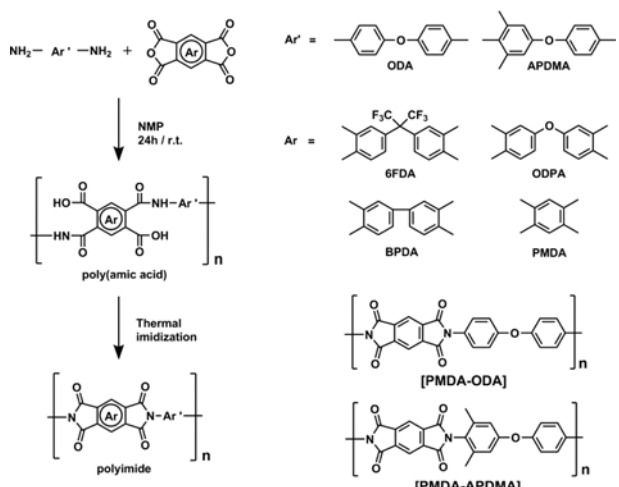
Results and Discussion

Synthesis and Characterization of Monomer. The new asymmetric diamine monomer, 4-(4-aminophenoxy)-2,6-dimethylaniline (APDMA), which contains a dimethyl groups, was composed in two steps, as shown in Scheme I. First, the monomer was synthesized from 4-amino-3,5-xylenol and 1-chloro-4-nitrobenzene by nucleophilic aromatic substitution reaction (SNAr). Second, nitro groups were reduced to amino groups by Pd/C catalyst and hydrazine. The chemical structures of diamines were identified by the ^1H , ^{13}C NMR spectroscopies, mass measurement, and FTIR investigation.

**Scheme I.** Synthesis of monomer.**Figure 1.** NMR spectra of APDMA (a) ^1H NMR and (b) ^{13}C NMR.

The ^1H and ^{13}C NMR spectra of APDMA are shown in Figure 1. The protons and carbon atoms were assigned without undesired structure. To be specific, the peaks of aromatic protons were observed at 6.79, 6.62, 6.60 ppm and the peak of protons on methyl groups was shown at 2.13 ppm in ^1H NMR. In addition, the characteristic signals of the amines were observed at 3.49 and 3.39 ppm. In the ^{13}C NMR, the peaks of aromatic carbons were assigned in the range of 115–150 ppm. In addition, the peak of benzylic carbons was shown in 17.8 ppm. Furthermore, intermediate DMNPA and final product APDMA were investigated by FTIR. The FTIR spectra are shown in Figure 2. The FTIR spectra of DMNPA showed characteristic bands at 1581, 1344 cm^{-1} assigned to N-O asymmetric and symmetric stretching. After reduction, the adsorption peak of the nitro group disappeared, and the amino group expanded N-H stretching bands located in 3347 and 3440 cm^{-1} . The observed results from NMR and FTIR studies were in good agreement with the expected structure of APDMA.

Synthesis and Characterization of Polymer. The new polyimides (PIs) were prepared by two-step thermal imidization method, as shown in Scheme II. First, diamine monomer

**Figure 2.** FTIR spectra of (a) DMNPA and (b) APDMA.**Scheme II.** Synthesis of polyimides.

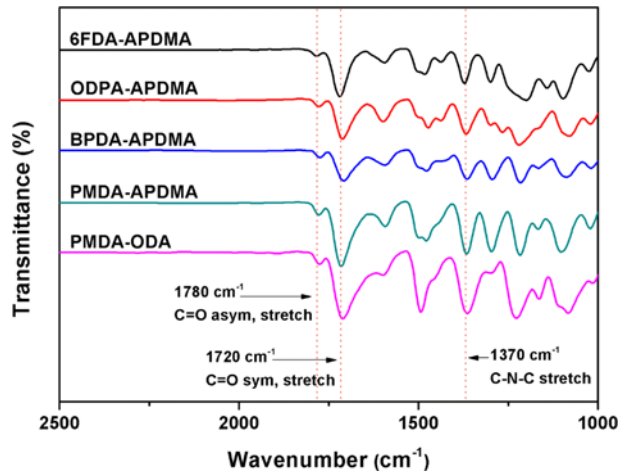
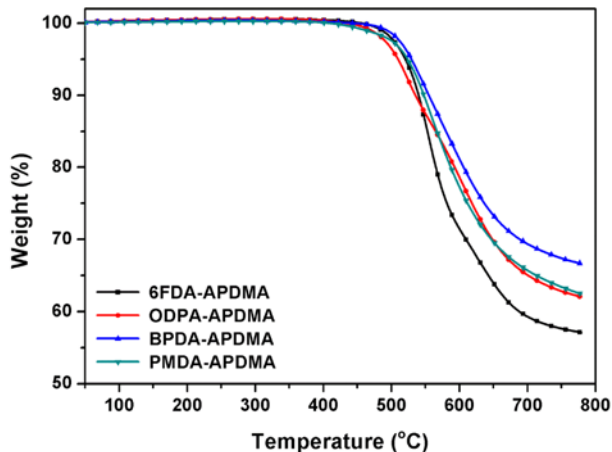
APDMA was dissolved in NMP with stoichiometric amounts of four types of dianhydride monomer, 6FDA, ODPA, BPDA and PMDA, respectively. The solution was stirred at room temperature for 24 h to obtain desired PAA through ring-opening polyaddition. Second process was that the PAA solutions were cast on the glass, quartz or silicon wafer, and imidized on the substrates by a sequential heating process under Ar atmosphere. The prepared PAA solid content was in the range of 16–20 wt% and their inherent viscosities were measured as 0.77–1.52 dL/g in NMP at 30 °C (Table I).

The chemical structure of PI films was characterized by FTIR spectroscopy. The FTIR spectra were shown in Figure 3. All PI films showed similar absorptions derived from imide structure. The characteristic imide group absorption peaks were observed around 1780 and 1720 cm^{-1} (imide carbonyl asymmetric and symmetric stretching, respectively) and 1370 cm^{-1} (C-N stretching vibration).⁹ These peaks of imide groups indicated the conversion of the poly(amic acids)s to the polyimides.

Table I. Inherent Viscosities of PAA and Thermal Properties of PI Films

Polymer	$[\eta]_{inh}^a$ (dL/g)	T_g^b (°C)		$T_{5\%}^c$ (°C)	$T_{10\%}^c$ (°C)	Char Yield ^d (%)
		DSC	DMA			
6FDA-APDMA	0.90	315	335	520	540	57
ODPA-APDMA	0.77	295	316	510	535	62
BPDA-APDMA	1.52	352	368	529	555	67
PMDA-APDMA	1.20	414	400	524	540	62
PMDA-ODA	0.78	-	-	581	596	57

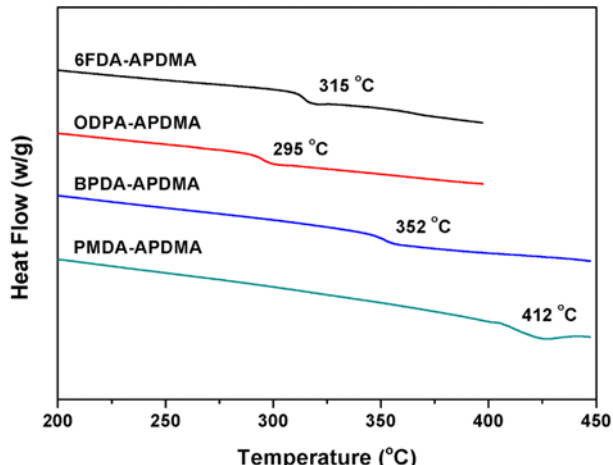
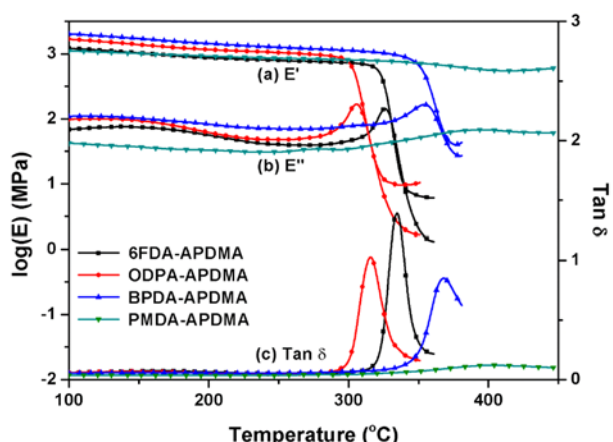
^aInherent viscosity of PAAs in 0.5 g/dL NMP solution at 30 °C. ^b T_g : glass transition temperature. ^c $T_{5\%}$, $T_{10\%}$: temperatures at 5% and 10% weight loss, respectively. ^dRemaining weight percentage after TGA analysis at 800 °C under N₂ atmosphere.

**Figure 3.** FTIR spectra of PI films.**Figure 4.** TGA curves of PI films (in nitrogen atmosphere, 10 °C/min).

Thermal Properties of Polyimides. The thermal properties of the PIs were investigated by TGA, DSC, and DMA measurement. The measured thermal properties are summarized in Table I. In the TGA measurement (Figure 4), the PI films were heated up to 800 °C at a heating rate of 10 °C/min in nitrogen atmosphere. All the PI films showed high decomposition temperature (T_d) without impressive weight loss up to

400 °C, and 5% weigh-loss temperatures ($T_{5\%}$) were measured around 510–581 °C. In addition, their char yield at 800 °C was more than 57%. In particular, the BPDA-APDMA film showed the highest $T_{5\%}$ and $T_{10\%}$ due to its linear and rigid-rod-like polymer chain structures.

The DSC and DMA curves are shown in Figures 5 and 6,

**Figure 5.** DSC curves of PI films (in nitrogen atmosphere, 10 °C/min).**Figure 6.** DMA curves of PI films (1 Hz, 3 °C/min): (a) storage modulus (E'), (b) loss modulus (E''), (c) $\tan \delta$.

respectively. The glass transition temperatures (T_g) of the PIs were determined by DSC and DMA. The DSC measurement was recorded at a heating rate of 10 °C/min in nitrogen atmosphere. In addition, the DMA measurement was carried out at a heating rate of 3 °C/min with a load frequency of 1 Hz in air, and T_g s were determined by the peak temperature of tan δ curve. The T_g s of the PI films were in the range of 295–414 °C and 316–400 °C, measured by DSC and DMA respectively. The glass transition temperatures were observed in the following order: PMDA > BPDA > 6FDA > ODPA. The observed tendency indicated the influence of chain rigidity by dianhydrides.¹⁰ The PMDA-APDMA, which retained a rigid backbone structure, represented the highest T_g , while ODPA-APDMA exhibited the lowest T_g value because of the effect of the flexible ether linkage and spatially extended molecular structure.

Optical Properties of Polyimides. The transparency in the visible region is one of important factors for optical application. The transmittances of PI films with a thickness of 10 μm on the quartz were measured by UV-visible spectrometer as shown in Figure 7. In addition, the optical properties of the PIs are summarized in Table II. The cutoff wavelengths of PIs

were in the range of 296–368 nm. In particular, 6FDA-APDMA film exhibited the lowest cutoff wavelength (296 nm) and the highest transmittance at 450 nm (87%). The outstanding optical properties of 6FDA-APDMA were obtained due to the bulky trifluoromethyl group of 6FDA component and dimethyl groups of APDMA unit. Steric hindrance from both of the functional groups inhibited the intermolecular chain packing and formation of charge transfer complex (CTC) between the polymer chains. Consequently, the 6FDA-APDMA showed optical cutoff of high energy and improved transparency.

To further investigate the improved transmittance of the film which derived from APDMA, the authors demonstrated theoretical calculation by density functional theory (DFT), employing model compounds of PMDA-APDMA and PMDA-ODA.¹¹ The resulting 3D molecular structures, orbital diagrams, and energy levels are depicted in Figure 8. The model compounds were composed by a repeating imide unit and calculated by B3LYP/6-31G function. The torsion angle of PMDA-APDMA between the phenylene ring and imide ring was 71.21° at ground state while the angle of PMDA-ODA was 40.96°. The steric hindrance of *ortho*-substituted methyl groups of PMDA-APDMA causes a greater torsion angle, which induces more transparent property derived from less intermolecular stacking than PMDA-ODA. In addition, the larger tilted backbone of PMDA-APDMA makes more localized HOMO orbital rather than that of PMDA-ODA. Moreover, the band gap energy of PMDA-APDMA (2.61 eV) is larger than that of PMDA-ODA (2.54 eV), which induces absorption cut at higher energy areas. In this regard, the molecular orbital calculation of model compounds showed a good consensus of experimental results.

The refractive indices and birefringence of the PI films were measured by the prism-coupling method using a laser beam at 637, 1306.5, and 1549.5 nm. The relationship between n_{av} and wavelength is shown in Figure 9. Table II exhibits the in-plane (n_{TE}), out-of-plane (n_{TM}), average refractive index (n_{av}), in-plane/out-of-plane birefringence (Δn), and thickness of the PI films used in refractive index measurement. The n_{TE} , n_{TM} , and n_{av} at 637 nm of PIs polymerized from APDMA monomer were in the range of 1.5689–1.6653, 1.5619–1.6540,

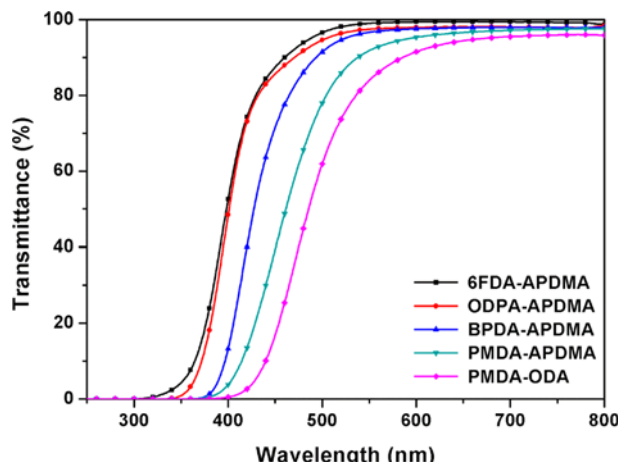


Figure 7. UV-vis absorption spectra of PI films (film thickness: ca. 10 μm).

Table II. Optical Properties of PI Films

Polymer	λ_{cutoff}^a (nm)	Transmittance ^b (%)	d^c (μm)	Refractive Indices and Birefringence at 637 nm ^d				n_{∞}^e	D^f ($\times 10^4$)
				n_{TE}	n_{TM}	n_{av}	Δn		
6FDA-APDMA	296	87	7.9	1.5689	1.5619	1.5666	0.0070	1.54	1.2097
ODPA-APDMA	322	86	8.8	1.6471	1.6374	1.6438	0.0097	1.60	1.5781
BPDA-APDMA	358	72	7.1	1.6653	1.6540	1.6615	0.0113	1.62	1.7619
PMDA-APDMA	353	39	7.5	1.6485	1.6142	1.6371	0.0343	1.59	1.5870
PMDA-ODA	368	17	6.5	1.7287	1.6445	1.7011	0.0842	1.65	1.8859

^aCut-off wavelength. ^bTransmittance at 450 nm and film thickness: ca. 10 μm. ^cFilm thickness for refractive index measurement. ^dMeasured at 637 nm, see measurements. ^eRefractive index at the infinite wavelength. ^fDispersion coefficient of refractive index obtained from the fitting by the simplified Cauchy formula ($n_{\lambda} = n_{\infty} + D\lambda^{-2}$).

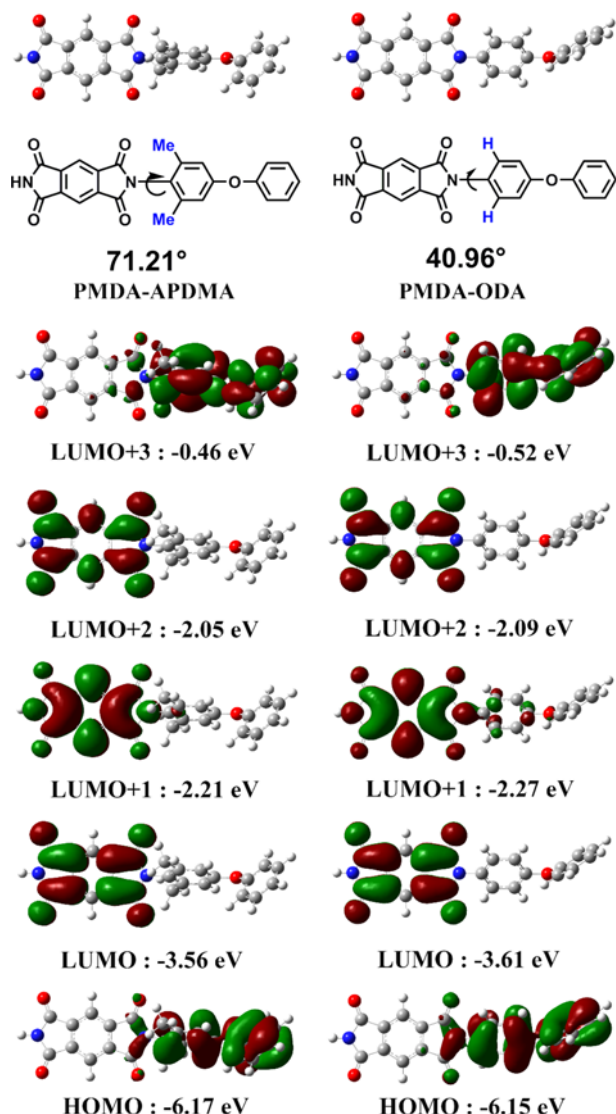


Figure 8. Molecular orbital diagrams of PMDA-APDMA and PMDA-ODA model compounds (calculated by B3LYP/6-31G function).

and 1.5666–1.6615, respectively. In particular, the n_{av} values of PIs were in the decreasing order BPDA > ODPA > PMDA > 6FDA, and the trend was determined by the chemical structure of polymer. In general, the refractive indices of polymer were affected by diverse factors, such as molecular geometry, chain flexibility or linearity of polymer backbone, and molecular packing. In this experiment, the molecular packing of in-plane orientation was reduced by the methyl group of APDMA monomer, consequently the 6FDA-APDMA polymer had the lowest refractive index (1.567) and birefringence (0.007) at 637 nm. While bulky dimethyl groups increase free volume of polymer and dense molecular packing generally results in high refractive index, ODPA-APDMA exhibited higher refractive indices than PMDA-APDMA in this study because PMDA-APDMA had a larger effect on the increase of free volume

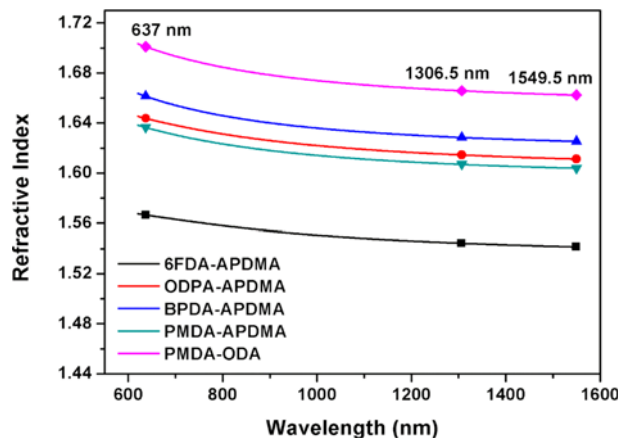


Figure 9. Wavelength dispersion of the refractive indices of PI films.

than that of ODPA-APDMA. In particular, in the comparison between PMDA-APDMA and PMDA-ODA containing rod-like dianhydride, PMDA-APDMA had lower refractive indices and birefringence than those of PMDA-ODA because the *ortho* position of amino groups made a large free molecular volume, which caused interruption of intermolecular packing.

Conclusions

In summary, we demonstrated the synthetic method of a new diamine monomer, APDMA, having *ortho*-substituted methyl groups on only one side of the phenylene ring of 4,4'-oxydianiline. The APDMA were polymerized with several aromatic dianhydrides, such as 6FDA, ODPA, BPDA, and PMDA, by a typical thermal imidization method. The glass transition temperatures of the synthesized PIs were in the region of 295–414 °C and the decomposition temperatures of those at 10% weight loss were in the region of 535–555 °C. In particular, 6FDA-APDMA exhibited high thermal stability due to decrease of intermolecular torsional potentials originated from *ortho*-substituted methyl groups of APDMA unit. In addition, the PIs from APDMA showed a highly improved transparency and lower refractive indices and birefringence values than the PIs from ODA. To be specific, the transparency of 6FDA-APDMA and ODPA-APDMA were over 85% at 450 nm, while PMDA-ODA's transparency was 17%. In addition, the refractive index and birefringence of 6FDA-APDMA at 637 nm was 1.5666 and 0.0070, respectively. These optical properties were able to be improved by simply introducing methyl substituents on diamine structure, which could induce less intermolecular stacking and rigid chain formation. This molecule design provides a new approach on development of improved organic materials.

Acknowledgments. This work was supported by a grant from the Korea Institute of Science and Technology (KIST) institutional program, Basic Science Research Program through

the National Research Foundation of Korea (NRF) funded by the Ministry of Education (2015R1A6A1A03031833), and by a grant from the Ministry of Trade, Industry & Energy of Korea (2MR4950).

References

- (1) (a) H. Choi, S.-J. Ko, Y. Choi, P. Joo, T. Kim, B. R. Lee, J.-W. Jung, H. J. Choi, M. Cha, and J.-R. Jeong, *Nat. Photonics*, **7**, 732 (2013). (b) M. S. Jung, J. H. Seo, M. W. Moon, J. W. Choi, Y. C. Joo, and I. S. Choi, *Adv. Energy Mater.*, **5**, 1400611 (2015). (c) S. Park, B. J. Park, S. Yun, S. Nam, S. K. Park, and K.-U. Kyung, *Opt. Express*, **22**, 23433 (2014). (d) K. I. Park, J. H. Son, G. T. Hwang, C. K. Jeong, J. Ryu, M. Koo, I. Choi, S. H. Lee, M. Byun, and Z. L. Wang, *Adv. Mater.*, **26**, 2514 (2014). (e) H. Souri, S. J. Yu, H. Yeo, M. Goh, J.-Y. Hwang, S. M. Kim, B.-C. Ku, Y. G. Jeong, and N.-H. You, *RSC Adv.*, **6**, 52509 (2016). (f) F. Di Giacomo, V. Zardetto, A. D'Epifanio, S. Pesce-telli, F. Matteocci, S. Razza, A. Di Carlo, S. Licoccia, W. M. Kes-sels, and M. Creatore, *Adv. Energy Mater.*, **5**, 1401808 (2015).
- (2) (a) N.-H. You, C.-C. Chueh, C.-L. Liu, M. Ueda, and W.-C. Chen, *Macromolecules*, **42**, 4456 (2009). (b) N. H. You, N. Fukuzaki, Y. Suzuki, Y. Nakamura, T. Higashihara, S. Ando, and M. Ueda, *J. Polym. Sci., Part A: Polym. Chem.*, **47**, 4428 (2009). (c) N. H. You, Y. Nakamura, Y. Suzuki, T. Higashihara, S. Ando, and M. Ueda, *J. Polym. Sci., Part A: Polym. Chem.*, **47**, 4886 (2009). (d) N. H. You, T. Higashihara, S. Ando, and M. Ueda, *J. Polym. Sci., Part A: Polym. Chem.*, **48**, 2604 (2010). (e) N. H. You, N. Fukuzaki, Y. Suzuki, Y. Nakamura, T. Higashihara, S. Ando, and M. Ueda, *J. Polym. Sci., Part A: Polym. Chem.*, **47**, 4428 (2009). (f) H. Yeo, J. Lee, M. Goh, B. C. Ku, H. Sohn, M. Ueda, N. and H. You, *J. Polym. Sci., Part A: Polym. Chem.*, **53**, 944 (2015). (g) Y.-H. Chou, N.-H. You, T. Kurosawa, W.-Y. Lee, T. Higashihara, M. Ueda, and W.-C. Chen, *Macro-molecules*, **45**, 6946 (2012).
- (3) (a) M. Nishihara, L. Christiani, A. Staykov, and K. Sasaki, *J. Polym. Sci., Part B: Polym. Phys.*, **52**, 293 (2014). (b) L. Christiani, S. Hilaire, K. Sasaki, and M. Nishihara, *J. Polym. Sci., Part A: Polym. Chem.*, **52**, 2991 (2014). (c) J. M. Salley and C. W. Frank, *Plastics Engineering-New York*, **36**, 279 (1996).
- (4) (a) H. Yeo, M. Goh, B.-C. Ku, and N.-H. You, *Polymer*, **76**, 280 (2015). (b) S. D. Kim, S. Y. Kim, and I. S. Chung, *J. Polym. Sci., Part A: Polym. Chem.*, **51**, 4413 (2013). (c) P. K. Tapaswi, M. C. Choi, S. Nagappan, and C. S. Ha, *J. Polym. Sci., Part A: Polym. Chem.*, **53**, 479 (2015).
- (5) (a) Y. Lu, G. Xiao, H. Chi, Y. Dong, and Z. Hu, *High Perform. Polym.*, **25**, 894 (2013). (b) Z. Huang and J. Zhao, *RSC Adv.*, **6**, 34825 (2016).
- (6) (a) D. H. Wang, J. K. Riley, S. P. Fillery, M. F. Durstock, R. A. Vaia, and L. S. Tan, *J. Polym. Sci., Part A: Polym. Chem.*, **51**, 4998 (2013). (b) J. Zhao, L. Peng, Y.-L. Zhu, A.-M. Zheng, and Y.-Z. Shen, *Polym. Chem.*, **7**, 1765 (2016).
- (7) (a) B. Ghanem, N. Alaslai, X. Miao, and I. Pinna, *Polymer*, **96**, 13 (2016). (b) Y. Guan, C. Wang, D. Wang, G. Dang, C. Chen, H. Zhou, and X. Zhao, *Polymer*, **62**, 1 (2015).
- (8) J. Lim, H. Yeo, M. Goh, B.-C. Ku, S. G. Kim, H. S. Lee, B. Park, and N.-H. You, *Chem. Mater.*, **27**, 2040 (2015).
- (9) J. Lim, D. G. Shin, H. Yeo, M. Goh, B. C. Ku, C. M. Yang, D. S. Lee, J. Y. Hwang, B. Park, and N. H. You, *J. Polym. Sci., Part B: Polym. Phys.*, **52**, 960 (2014).
- (10) D.-J. Liaw, K.-L. Wang, Y.-C. Huang, K.-R. Lee, J.-Y. Lai, and C.-S. Ha, *Prog. Polym. Sci.*, **37**, 907 (2012).
- (11) M. J. Frisch, *et al.*, Gaussian 03 (Revision C.01), Gaussian, Inc., Wallingford CT (2004).